RSC Advances

PAPER

View Article Online
View Journal | View Issue

Cite this: *RSC Adv.*, 2022, **12**, 24633

Fluorescent cellulose nanocrystals based on AIE luminogen for rapid detection of Fe^{3+} in aqueous solutions

Xiu Ye, [ab] Dongyang Zhang,[c] Sai Wang,[a] Peng Zhou*[a] and Pengli Zhu*[b]

Received 11th July 2022
Accepted 5th August 2022

DOI: 10.1039/d2ra04272j

rsc.li/rsc-advances

Previously, we found that aggregation-induced emission (AIE) luminogen tetraphenylethylene (TPE) based fluorescent cellulose nanocrystals (TPE-CNCs) showed excellent AIE-active fluorescence properties and high selectivity and sensitivity for detecting nitrophenol explosives in aqueous solutions. Here, we further develop the application of TPE-CNCs for fluorescence detection of Fe^{3+} in aqueous solutions. The fluorescence of TPE-CNC aqueous suspensions is rapidly quenched (response time less than 10 s) due to the electron-transfer process between TPE and Fe^{3+} upon addition of Fe^{3+}. TPE-CNCs have high sensitivity and selectivity toward Fe^{3+} over a broad pH range from 4 to 10. The limit of detection is determined to be 264 nM, which is below the World Health Organization (WHO) recommendations (5.36 μM) for Fe^{3+}. Given the superior properties of TPE-CNCs, it has huge potential to be applied as a rapid and visual evaluation tool for drinking water quality. Collectively, we explore and develop fluorescent cellulose nanocrystals for multi-functional applications and TPE-CNCs can be used for practical applications in sensing, sewage treatment and bioimaging.

Introduction

Iron (Fe) is a ubiquitous element found in rock, soil, water and organisms. As an essential trace element, it plays crucial roles in many biological processes in humans, animals and plants. Both ferric ion (Fe^{3+}) deficiency and overload may cause several serious human disorders, such as Alzheimer's disease, loss of hair, lethargy, infectious diseases, weakness, neurodegenerative disorders, hemochromatosis, liver damage and anemia.[1,2] Moreover, Fe^{3+} accumulation over time in the human body leads to various malignancies, of which cardiac and hepatic complications are two typical diseases of severe iron overload.[3] Given the importance of Fe^{3+} in living systems, developing sensors for Fe^{3+} detection have received considerable critical attention. Thus, simple, fast, sensitive, and accurate detection of Fe^{3+} is great needed for human safety and health.[4] To date, among various sensors, fluorescent Fe^{3+} sensors have served as a great model due to their high sensitivity, simplicity, convenience, and diversity.[5]

Organic dye-based fluorescent probes have been extensively studied due to their diversity and modifiability. However, most organic dyes are intrinsic hydrophobic, low stability, poor biocompatibility, and environment-unfriendly.[6] Moreover, these organic dyes also suffer from aggregation issues, leading to fluorescence quenching even at low concentrations. Nowadays, novel fluorescent nanomaterial probes exhibit radically different properties compared to organic fluorophores, such as fascinating optical properties, easy functionalization, and excellent biocompatibility.[7] Cellulose nanocrystals (CNCs), represents as a novel fascinating bio-based nanomaterial with many excellent features. For example, naturally abundant, low-cost, renewable, easy chemical modification, environmentally benign, biocompatible and biodegradable.[8] Thus, CNCs have attracted extensive interest from researchers in both industry and academia due to their outstanding properties and potential applications. Previously, through surface modification of CNCs, functionalized CNCs have been widely developed for various applications, such as reinforcing filler for polymers, paper-making industry, biomedical, food industry, water treatment, sensor, *etc.*[9,10] Additionally, by means of grafting fluorescent dyes onto CNCs surface, fluorescent labeled CNCs have been explored for drug delivery, bioimaging, and sensing in recent years.[11–13] Fluorescent labeled CNCs show excellent fluorescent properties and water dispersibility, making them outstanding candidates for fluorescence detection of various analytes.[14–16] Fluorescent labeled CNCs have also been reported as fluorescent probes for metal ions detection. For example, Zhang *et al.* reported pyrene labeled CNCs (Py-CNC) for Fe^{3+} detection in aqueous solution.[17] Moreover, Song *et al.* reported 1, 8-naphthalimide labeled CNCs (FCNCs) for Pb^{2+} detection in aqueous

[a]*Institute of Intelligent Manufacturing Technology, Shenzhen Polytechnic, Shenzhen 518055, China. E-mail: zhoupeng85723@163.com; Tel: +86-755-26731946*

[b]*Shenzhen Institutes of Advanced Electronic Materials, Shenzhen Institutes of Advanced Technology, Chinese Academy of Sciences, Shenzhen 518055, China. E-mail: pl.zhu@siat.ac.cn*

[c]*Institute of Critical Materials for Integrated Circuits, Shenzhen Polytechnic, Shenzhen, 518055, China*

solution.[18] More recently, Zhang *et al.* reported 7-amino-4-methylcoumarin labeled CNCs (A-ECNC) for quantitative Cu^{2+}detection in aqueous solution.[19]

To date, most fluorescent labeled CNCs are developed by using classic organic dyes which always suffer fluorescence quenching upon aggregation, named as aggregation-caused quenching (ACQ) effect.[20,21] Conversely, aggregation-induced emission (AIE) is completely opposite to ACQ, which is non-emissive in dilute solutions, but has intense fluorescence in the solid or aggregated state.[22] Previously, we first synthesized AIE-active cellulose nanocrystals (TPE-CNCs), with excellent fluorescence properties and high selectivity and sensitivity for nitrophenol explosives detection in complete aqueous solutions.[16] In the previous studies, AIE-active TPE polymers and derivatives have been effectively utilized for metal ions detection.[23–26] Surprisingly, AIE-active CNCs has still not been investigated for metal ions detection. Since coordination-induced complexation between the TPE unit of TPE-CNCs and metal ions may lead to fluorescence response.[27] In this work, we employed TPE-CNCs aqueous suspensions for detecting Fe^{3+}. It is widely known that Fe^{3+} is a classic fluorescence quencher because of its paramagnetic nature.[28] The fluorescence of TPE-CNCs aqueous suspensions was efficiently quenched when Fe^{3+} was combined TPE-CNCs. Thus, we envisioned that TPE-CNCs could serve as an excellent probe for Fe^{3+} with high selectivity and sensitivity in aqueous solution.

Experimental section

Materials

Cellulose nanocrystals were purchased from Shanghai ScienceK Ltd, China, which were synthesized by sulphuric acid hydrolysis of microcrystal cellulose. 4-(1,2,2-Triphenylvinyl)benzoicacid (TPE-COOH) was purchased from Xi'an Qiyue Biotechnology Co. Ltd, China. Epichlorohydrin, sodium hydroxide (NaOH), ammonium hydroxide ($NH_3 \cdot H_2O$), dimethyl sulfoxide (DMSO), 1-(3-dimethylaminopropyl)-3-ethylcarbodiimide hydrochloride (EDC), 4-dimethylaminopyridine (DMAP), as well as NaCl, $MgCl_2 \cdot 6H_2O$, $CaCl_2$, $ZnCl_2$, $Pb(NO_3)_2$, $HgCl_2$, $FeSO_4 \cdot 7H_2O$, $FeCl_3 \cdot 6H_2O$, $CuSO_4 \cdot 5H_2O$, $CoCl_2 \cdot 6H_2O$, $BaCl_2 \cdot 2H_2O$, $AlCl_3$, $CdCl_2$ and $MnSO_4$ were purchased from Sinopharm Chemical Reagent Co. Ltd, China. All reagents were analytical grade and received directly without any further purification. The deionized water was used to prepare all aqueous solutions.

Preparation of TPE-CNCs

TPE-CNCs was synthesized using the following procedure as previously described (Scheme 1).[16] First, epoxy-activated CNCs was synthesized with CNCs and epichlorohydrin under alkaline conditions. Second, epoxy group combined CNCs opened the epoxy ring to introduce amino groups for derivatization reactions. Finally, TPE-CNCs was synthesized with CNC–NH_2 and TPE–COOH by condensation reaction. TPE-CNCs suspension was concentrated and sonicated, and stored in refrigerator at 4 °C before measurements.

Instruments and characterizations

Fluorescence spectra were obtained on a Shimadzu RF-5300pc spectrofluorophotometer with the excitation/emission slit width of 6/4 nm, the excitation wavelength of 330 nm, and the emission wavelength recorded in the range of 350–600 nm. The pH of the aqueous suspensions was measured with a digital pH meter (Sanxin-MP521, Shanghai, China).

Metal ion sensing experiments of TPE-CNCs

To investigate the selectivity of TPE-CNCs, TPE-CNCs aqueous suspension (4 mL, 0.05 wt%) and different metal ions (Na^+, Mg^{2+}, Ca^{2+}, Zn^{2+}, Pb^{2+}, Hg^{2+}, Fe^{2+}, Fe^{3+}, Cu^{2+}, Co^{2+}, Ba^{2+}, Al^{3+}, Cd^{2+} and Mn^{2+}) solutions (300 μM) were mixed, separately. Then, the mixture was filled in a quartz optical cell. To evaluate the sensitivity of TPE-CNCs for Fe^{3+}, a series of different concentration of Fe^{3+} standard solutions (1, 2, 5, 10, 15, 20, 30, 40, 60, 80, 100, 200, 300, 500 μM) were added to TPE-CNCs aqueous suspensions (0.05 wt%). Before measurement, the mixtures were incubated for 20 min to ensure the reaction reached equilibrium. For all fluorescence measurements, the data of fluorescence spectra were collected under excitation/emission slit width of 6/4 nm, the excitation wavelength at 330 nm, and the maximum emission wavelength at 421 nm.

For the time response experiment, after adding Fe^{3+} (300 μM) into TPE-CNCs aqueous suspensions (0.05 wt%), the data of fluorescence spectra were collected after mixing time point at 0, 5, 30, 60, 120, 180 s. To investigate the pH-dependent response of TPE-CNCs for Fe^{3+}, the suspension pH was titrated from 3.0 to 12.0 using either 0.1 M HCl or NaOH aqueous solutions, and then the fluorescence spectra were recorded after 5 min. All experiments were performed at room temperature.

Results and discussion

Detection of Fe^{3+} using TPE-CNCs

To evaluate the selectivity of TPE-CNCs aqueous suspensions for Fe^{3+}, we characterized the fluorescence emission response of TPE-CNCs aqueous suspensions (0.05 wt%) against different metal ions (300 μM, including Na^+, Mg^{2+}, Ca^{2+}, Zn^{2+}, Pb^{2+}, Hg^{2+}, Fe^{2+}, Fe^{3+}, Cu^{2+}, Co^{2+}, Ba^{2+}, Al^{3+}, Cd^{2+} and Mn^{2+}, respectively). The fluorescence intensity ratio I/I_0 values of TPE-CNCs aqueous suspensions with exogenous metal ions are shown in Fig. 1a, where I and I_0 represent the emission intensity of TPE-CNCs aqueous suspensions at 421 nm with and without metal ions, respectively. The data showed that Fe^{3+} had the lowest I/I_0 value of ~0.07, indicating an apparent quenching effect of TPE-CNCs, whereas the other metal ions did not exhibit such behavior under the same conditions. Subsequently, to evaluate the specificity of probe TPE-CNCs toward Fe^{3+}, the interference experiment was performed by adding of Fe^{3+} (300 μM) to TPE-CNCs aqueous suspensions with other coexisting ions (300 μM). As shown in Fig. 1b, the fluorescence quenching of Fe^{3+} with other coexisting ions was similar to that of only Fe^{3+}, and no obvious interferences were observed. Moreover, TPE-CNCs aqueous suspensions showed good discrimination between Fe^{3+} and Fe^{2+}. Overall, these results showed remarkably high

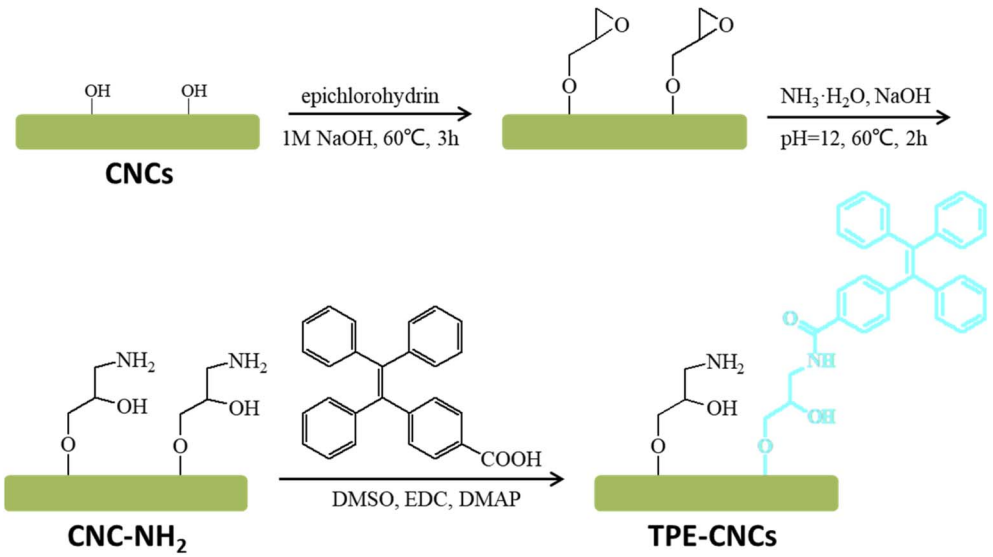

Scheme 1 Synthesis route of TPE-CNCs.

selectivity and specificity of TPE-CNCs aqueous suspensions toward Fe^{3+}.

In addition to selectivity, sensitivity is a vital parameter for appraising the performance of fluorescent probes. To evaluate the sensitivity for quantitative detection of Fe^{3+}, the fluorescence emission spectra of TPE-CNCs aqueous suspension (0.05 wt%) after adding Fe^{3+} (1–500 μM) were recorded. As shown in Fig. 2a, the fluorescence emission spectra of TPE-CNCs aqueous suspension showed high fluorescence intensity at 421 nm upon excitation at 330 nm. Titration experiments showed that the fluorescence intensity of TPE-CNCs decreased with increasing Fe^{3+} concentration. In addition, the fluorescence color changed from blue-white to colorless, as shown in the inset of Fig. 2b. The fluorescence quenching efficiency was sufficient to achieve more than 92% when the concentration of Fe^{3+} increased to 500 μM, indicating that probe TPE-CNCs has high sensitivity toward Fe^{3+}. The fluorescence quenching behavior of TPE-CNCs sensor with Fe^{3+} was further examined using Benesi–Hildebrand and Stern–Volmer plot. The binding stoichiometry and the association constant between TPE-CNCs and Fe^{3+} was determined using the Benesi–Hildebrand equation.[29]

$$1/(I_0 - I) = 1/[K[Fe^{3+}]\ (I_0 - I)] + 1/(I_0 - I) \quad (1)$$

where I_0 and I are the fluorescence intensity of TPE-CNCs aqueous suspension at 421 nm without and with Fe^{3+}, respectively, K is the association constant, and $[Fe^{3+}]$ was the Fe^{3+} concentration. As shown in Fig. 3a, the plot of $1/(I_0 - I)$ *versus* $1/[Fe^{3+}]$ shows a good linear correlation, with a correlation coefficient (R^2) of 0.968, indicating the 1 : 1 binding stoichiometry between TPE-CNCs and Fe^{3+}. The estimated value of association constant K was determined to be $2.034 \times 10^5\ M^{-1}$, which indicates a strong binding affinity of TPE-CNC towards Fe^{3+}.

The binding stoichiometry was also confirmed using Stern–Volmer plot. The Stern–Volmer analysis of fluorescence

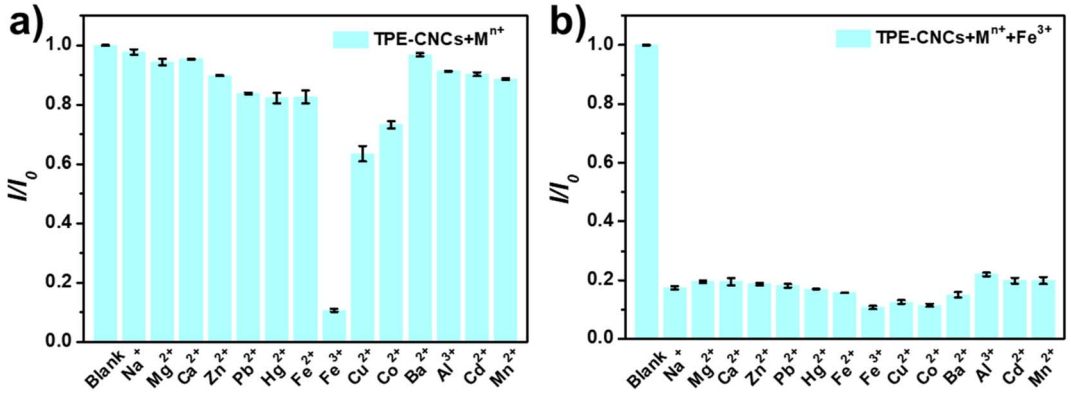

Fig. 1 (a) Fluorescence response of TPE-CNCs aqueous suspensions (0.05 wt%) to various metal ions (300 μM). (b) Fluorescence response of TPE-CNCs aqueous suspensions (0.05 wt%) to Fe^{3+} in the presence of competition metal ions (300 μM) ($\lambda_{ex} = 330$ nm, Ex/Em = 6/4) (I_0 and I are the fluorescence intensities of TPE-CNCs without and with metal ions).

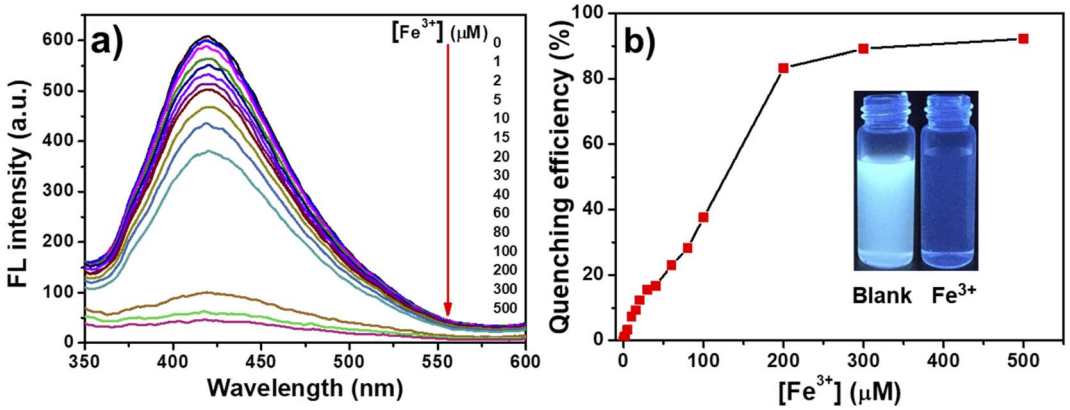

Fig. 2 (a) Fluorescence spectra and (b) quenching efficiency of TPE-CNCs aqueous suspensions (0.05 wt%) with different concentrations of Fe^{3+}.

quenching behavior of TPE-CNCs sensor with Fe^{3+} is given by the following equation.[30]

$$I_0/I = 1 + K_{SV}[Fe^{3+}] \quad (2)$$

where I_0 and I were the fluorescence intensity of TPE-CNCs aqueous suspension at 421 nm without and with Fe^{3+}, respectively, K_{SV} is the Stern–Volmer quenching constant, $[Fe^{3+}]$ is the Fe^{3+} concentration. As shown in Fig. 3b, the fluorescence intensity ratio (I/I_0) of TPE-CNCs and the concentration of Fe^{3+} can be finely fitted to the Stern–Volmer equation in the range of 0–30 μM, indicating that the quenching was static instead of dynamic.[31] The Stern–Volmer plot with K_{SV} of 6000 M^{-1} and R^2 of 0.993 suggested the high fluorescence quenching efficiency of Fe^{3+} towards TPE-CNCs. The limit of detection (LOD) of TPE-CNCs for Fe^{3+} was obtained based on the following equation.[32]

$$LOD = 3\sigma/S \quad (3)$$

where σ and S are the standard deviation of the I_0/I values and the slope of the linear line, respectively. The detection limit was estimated to be 265 nM, which is considerably lower than the guideline for the Fe^{3+} concentration (5.36 μM) in drinking water suggested by the World Health Organisation (WHO).[33] These results suggested that TPE-CNCs could be sensitive to detect Fe^{3+} in water. Moreover, adsorbents based on modified CNCs were the recent trend in developing new wastewater treatment methods.[34] This suggested that TPE-CNCs could also be applied in water treatment for Fe^{3+} removal.

Respond time and pH stability

The response time and pH stability are two vital indicators for evaluating the practical application value of fluorescent probes. We investigated the fluorescence response time of TPE-CNCs aqueous suspension for detecting Fe^{3+} by dynamically monitoring the fluorescence quenching efficiency of the process. As shown in Fig. 4a, the fluorescence intensity of TPE-CNCs aqueous suspension was immediately quenched within 10 s after the addition of Fe^{3+}, and then was stable after 30 s. The short response time suggests that TPE-CNCs aqueous suspension can be efficiently used for Fe^{3+} detection, and has significant implications in practical applications. More importantly, the fluorescence turn-off phenomenon can be observed easily with naked eyes under ultraviolet light (365 nm). To confirm whether TPE-CNCs probe can detect Fe^{3+} toward different pH conditions, the influence of pH range from 3 to 12 on the fluorescent intensity of the probe TPE-CNCs aqueous

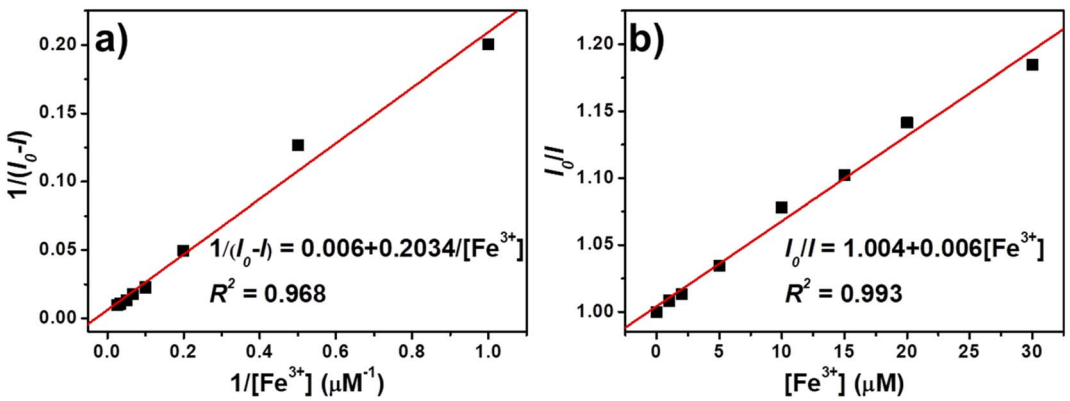

Fig. 3 (a) Benesi–Hildebrand and (b) Stern–Volmer plot of TPE-CNCs aqueous suspension fluorescence quenching by Fe^{3+}.

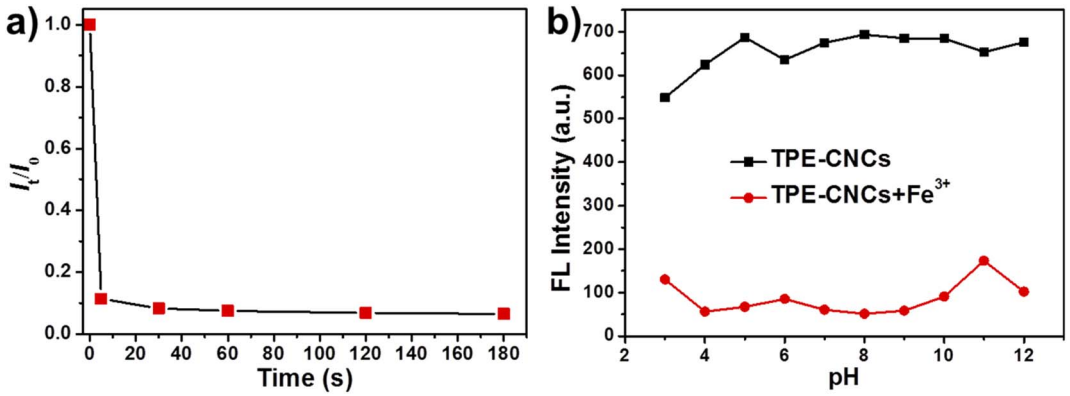

Fig. 4 (a) The response time of TPE-CNCs aqueous suspensions (0.05 wt%) to Fe^{3+} (300 μM). (b) Effect of pH on TPE-CNCs aqueous suspensions for Fe^{3+} detection.

Table 1 Comparision of various fluorescence probes for Fe^{3+} detection

Sample	Solvent	K (10^5 M^{-1})	LOD (μM)	Ref.
TPE-CNCs	H_2O	2.034	0.265	This work
Py-CNCs	H_2O	0.5375	1	17
Oligothiophene Schiff base	DMSO/H_2O	13.4	2.74	35
Quinoline Schiff base	MeOH	0.722	0.048	36
Rhodamine B derivative	MeOH/H_2O	24.6	0.396	37
DQC	DMSO/H_2O	7.7×10^{-4}	0.16	38
Chitosan-MBP	DMF/H_2O	0.171	1.2	39
CDs-curcumin	MeOH	1.07	0.018	40
TPE derivative	THF/H_2O	16.3	2.69×10^{-3}	41

suspension was evaluated. The fluorescence intensity at different pH values are shown in Fig. 4b. The fluorescent intensity of TPE-CNCs aqueous suspension (0.05 wt%) was strong, and remained basically unchanged at 421 nm over pH range from 4 to 12, suggesting that the fluorescent property of TPE-CNCs aqueous suspension was stable and pH-independent over pH range from 4 to 12. In the presence of Fe^{3+} (300 μM), the fluorescent intensity of TPE-CNCs aqueous suspension had a strong quenching effect caused by Fe^{3+}, and the quenching effect was relatively stable in the pH range 4–10. When the pH value was less than 4 and larger than 10, TPE-CNCs could not be accurately detected because of the hydrolysis of Fe^{3+} and the instability of TPE-CNCs in aqueous suspension. These results suggested that TPE-CNCs aqueous suspension could quickly detect Fe^{3+} effectively over a broad pH range, which had great significance in practical application.

Furthermore, we compared the performance of TPE-CNCs probe with other reported fluorescence probes for Fe^{3+} detection, as summarized in Table 1. It can be found that although many probes have high selectivity and recognition ability for Fe^{3+} detection, most probes have limitations such as poor water solubility. TPE-CNCs exhibited better or comparable

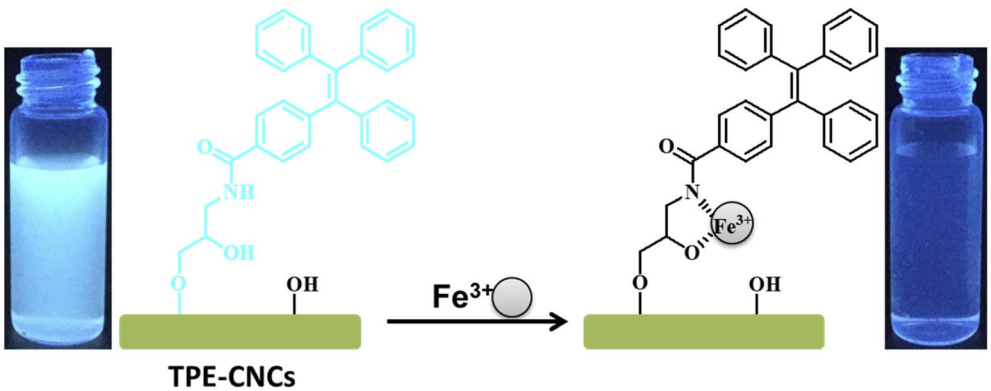

Scheme 2 Proposed binding mode of TPE-CNCs with Fe^{3+}.

performance, including good water dispersion, high association constant and low detection limit.

Possible sensing mechanism of TPE-CNCs to Fe^{3+}

It is well known that energy- or electron-transfer processes between fluorophore and metal ion can lead to fluorescence enhancement or quenching.[42] The recognition unit of TPE-CNCs could complex with Fe^{3+} selectively due to the specific structure. The chelation between Fe^{3+} and TPE-CNCs is facilitated by the coordination from N–H group and O–H group. Moreover, N–H group has strong binding affinity to metal ions. Fe^{3+} is an efficient paramagnetic quencher with an unfilled d shell, which can participate in energy- or electron transfer of many fluorophores.[17,43] Then, the fluorescence quenching of TPE-CNCs occurred by electron-transfer process between TPE and Fe^{3+}. Based on previously described results, we proposed a possible binding mode between TPE-CNCs and Fe^{3+} as shown in Scheme 2. When Fe^{3+} existed, the TPE units of TPE-CNCs banded Fe^{3+} with "O" and "N" atom, the electron-transfer process between TPE and Fe^{3+} caused fluorescence quenching of TPE-CNCs.

Conclusions

In this study, fluorescent cellulose nanocrystals based on AIE luminogen (TPE-CNCs) was developed the application for highly selective and sensitive detection of Fe^{3+} in aqueous suspension. TPE-CNCs showed rapid efficient fluorescence quenching towards Fe^{3+}, which occurred by a static mechanism *via* the electron-transfer process upon the coordination induced complexation between TPE and Fe^{3+}. Based on the Benesi–Hildebrand and Stern–Volmer method, the binding stoichiometry and association constant between TPE-CNCs and Fe^{3+} were found to be 1 : 1 and $2.034 \times 10^5\ M^{-1}$, respectively. The limit of detection was determined as 264 nM, which was considerably lower than the guideline of drinkable water proposed by the WHO. In general, TPE-CNCs showed several excellent advantages compared to many other reported Fe^{3+} probes, such as good water dispersion, short response time (less than 10 s), high selectivity and sensitivity, high association constant, low LOD, and detecting Fe^{3+} over a broad pH range from 4 to 10. This novel fluorescent cellulose nanocrystals (TPE-CNCs) can be used for detection of nitrophenol explosives and Fe^{3+}. Our work may help to extend fluorescent cellulose nanocrystals for multifunctional applications. Therefore, we believe TPE-CNCs will hopefully find many potential applications in sensing, sewage treatment and bioimaging.

Author contributions

X. Ye designed and performed the experiments, and drafted the manuscript; D. Zhang and S. Wang provided advices and performed the experiments; P. Zhou and P. Zhu advised the work; all the authors discussed the results and approved the manuscript.

Conflicts of interest

The authors declare no conflict of interest.

Acknowledgements

The authors would like to acknowledge the support from Shenzhen Science and Technology Innovation Commission (Grant No. JCYJ20190809111603608), Post-doctoral Foundation Project of Shenzhen Polytechnic (Grant No. 6021330019K0 and 6021330011K0), Innovation Project of Shenzhen Polytechnic (Grant No. CXGC2021C0003), Natural Science Foundation of Guangdong Province, China (Grant No. 2020A1515011194 and 2019B1515120013) and Guangdong Provincial General University Innovation Team Project (Grant No. 2020KCXTD047).

References

1 M. E. Besheli, R. Rahimi, D. F. Farahani and V. Safarifard, *Inorg. Chim. Acta*, 2019, **495**, 118956.
2 K. Joppe, A.-E. K. Roser, A.-E. Roser, F. Maass and P. Lingor, *Front. Neurosci.*, 2019, 13.
3 A. Siddique and K. V. Kowdley, *Nanomaterials*, 2012, **35**, 876–893.
4 S. Chakraborty, M. Mandal, M. Ray and S. Rayalu, *Inorg. Chem. Commun.*, 2020, **121**, 108189.
5 S. K. Sahoo and G. Crisponi, *Molecules*, 2019, **24**, 3267.
6 Y. Li, Z. Cai, S. Liu, H. Zhang, S. Wong, J. W. Y. Lam, R. T. K. Kwok, J. Qian and B. Z. Tang, *Nat. Commun.*, 2020, **11**, 1225.
7 P. Reineck and B. C. Gibson, *Adv. Opt. Mater.*, 2017, **5**, 1600446.
8 V. Thakur, A. Guleria, S. Kumar, S. Sharma and K. Singh, *Mater. Adv.*, 2021, **2**, 1872–1895.
9 A. K. Rana, E. Frollini and V. K. Thakur, *Int. J. Biol. Macromol.*, 2021, **182**, 1554–1581.
10 T. Aziz, H. Fan, X. Zhang, F. Haq, A. Ullah, R. Ullah, F. U. Khan and M. Iqbal, *J. Polym. Environ.*, 2020, **28**, 1117–1128.
11 S. Raja, A. E. I. Hamouda, M. A. S. de Toledo, C. Hu, M. P. Bernardo, C. Schalla, L. S. F. Leite, E. M. Buhl, S. Dreschers, A. Pich, M. Zenke, L. H. C. Mattoso and A. Sechi, *Biomacromolecules*, 2021, **22**, 454–466.
12 R. Li, Y. Liu, F. Seidi, C. Deng, F. Liang and H. Xiao, *Adv. Mater.*, 2022, **9**, 2101293.
13 R. Nasseri, C. P. Deutschman, L. Han, M. A. Pope and K. C. Tam, *Mater. Today Adv.*, 2020, **5**, 100055.
14 W. Yuan, C. Wang, S. Lei, J. Chen, S. Lei and Z. Li, *Polym. Chem.*, 2018, **9**, 3098–3107.
15 L. Zhang, S. Lyu, Q. Zhang, Y. Wu, C. Melcher, S. C. Chmely, Z. Chen and S. Wang, *Carbohydr. Polym.*, 2019, **206**, 767–777.
16 X. Ye, H. Wang, L. Yu and J. Zhou, *Nanomaterials*, 2019, **9**, 707.
17 L. Zhang, Q. Li and J. Zhou, *Macromol. Chem. Phys.*, 2012, 1612–1617.
18 R. Song, Q. Zhang, Y. Chu, L. Zhang, H. Dai and W. Wu, *Cellulose*, 2019, **26**, 9553–9565.

19 Y. Zhang, X. Ma, L. Gan, T. Xia, J. Shen and J. Huang, *Cellulose*, 2018, **25**, 5831–5842.
20 J. W. Grate, K. Mo, Y. Shin, A. Vasdekis, M. G. Warner, R. T. Kelly, G. Orr, D. Hu and M. J. Wilkins, *Bioconjugate Chem.*, 2015, **26**, 593–601.
21 J. Huang, C. Li and D. G. Gray, *ACS Sustainable Chem. Eng.*, 2013, **1**, 1160–1164.
22 X. Ma, R. Sun, J. Cheng, J. Liu, F. Gou, H. Xiang and X. Zhou, *J. Chem. Educ.*, 2016, **93**, 345–350.
23 D. D. La, S. V. Bhosale, L. A. Jones and S. V. Bhosale, *ACS Appl. Mater. Interfaces*, 2018, **10**, 12189–12216.
24 Y. Liu, Z. Wang, W. Qin, Q. Hu and B. Z. Tang, *Chin. J. Polym. Sci.*, 2017, **35**, 365–371.
25 D. N. Nadimetla and S. V. Bhosale, *New J. Chem.*, 2021, **45**, 7614–7621.
26 Y. Zheng, H. Wang and J. Jiang, *Dyes Pigm.*, 2020, **173**, 107929.
27 P. Alam, N. L. C. Leung, J. Zhang, R. T. K. Kwok, J. W. Y. Lam and B. Z. Tang, *Coord. Chem. Rev.*, 2021, **429**, 213693.
28 L. Fu, J. Mei, J. Zhang, Y. Liu and F. Jiang, *Luminescence*, 2013, **128**, 602–606.
29 R. Wang and Z. Yu, *Acta Phys.-Chim. Sin.*, 2007, **23**, 1353–1359.
30 M. H. Gehlen, *J. Photochem. Photobiol., C*, 2020, **42**, 100338.
31 L. Wang, K. H. Li, Y. Yang, D. Zhang, M. Wu, B. Pan and B. Xing, *Water Res.*, 2017, **122**, 337–344.
32 B. Wang, Y. Lin, H. Tan, M. Luo, S. Dai, H. Lu and Z. Huang, *Analyst*, 2018, **143**, 1906–1915.
33 WHO, *World Health Organization*, Geneva, Switzerland, 1997.
34 R. Z. Khoo, W. S. Chow and H. Ismail, *Cellulose*, 2018, **25**, 4303–4330.
35 L. Lan, Q. Niu, Z. Guo, H. Liu, H. Liu and T. Li, *Sens. Actuators, B*, 2017, **244**, 500–508.
36 B. Li, J. Tian and D. Zhang, *Luminescence*, 2017, **32**, 1567–1573.
37 X. Bao, X. Cao, X. Nie, Y. Xu, W. Guo, B. Zhou, L. Zhang, H. Liao and T. Pang, *Sens. Actuators, B*, 2015, **208**, 54–66.
38 P. Madhu and P. Sivakumar, *J. Mol. Struct.*, 2019, **1193**, 378–385.
39 C. Li, L. Marin and X. Cheng, *Int. J. Biol. Macromol.*, 2021, **186**, 303–313.
40 F. Yan, F. Zu, J. Xu, X. Zhou, Z. Bai, C. Ma, Y. Luo and L. Chen, *Sens. Actuators, B*, 2019, **287**, 231–240.
41 D. Wang, C. Ma, X. Zhou, W. Long, M. Liu, X. Zhang and Y. Wei, *Colloid Interface Sci. Commun.*, 2021, **40**, 100358.
42 B. Daly, J. Ling and A. P. de Silva, *Chem. Soc. Rev.*, 2015, **44**, 4203–4211.
43 Z. Huang, W. Song, Y. Li, L. Wang, N. K. Pandey, L. Chudal, M. Wang, Y. Li, L. Zhao, W. Yin and W. Chen, *J. Mater. Chem. C*, 2020, **8**, 12935–12942.